Environ. Sci. Technol. 1997, 31, 2244–2251

SFUND RECORDS CTR
46849

Proton Generation by Dissolution of Intrinsic or Augmented Aluminosilicate Minerals for in Situ Contaminant Remediation by Zero-Valence-State Iron

ROBERT M. POWELL*,† AND ROBERT W. PULS‡

Powell & Associates Science Services, 8310 Lodge Haven Street, Las Vegas, Nevada 89123-2632, and National Risk Management Research Laboratory, Robert S. Kerr Environmental Research Center, U.S. Environmental Protection Agency, Ada, Oklahoma 74821

Metallic, or zero-valence-state, iron is being incorporated into permeable reactive subsurface barriers for remediating a variety of contaminant plume types. The remediation occurs via reductive processes that are associated with surface corrosion of the iron metal. Reaction rates for these processes vary widely with both the form of iron and the contaminant but have previously been shown to increase when certain aquifer materials are present in the mix. Knowledge of such geochemical effects is important for planning an in situ remediation, as well as understanding the transport and fate of the contaminant within the barrier. The increase in reaction rate has been hypothesized to be due to the presence of aluminosilicate minerals in some aquifer materials that can dissolve and participate in the reaction sequences. Current results show that a variety of aluminosilicate minerals, including kaolinite, montmorillonite, and a range of feldspars, can undergo dissolution in these disequilibrium systems and provide protons as electron acceptors at a rate sufficient to maintain and/or enhance the reactions. The proposed reactions are illustrated for aluminosilicate dissolution and chromate reduction. A potential benefit for TCE dechlorination is also depicted. These aluminosilicates may occur naturally in the aquifer geology and become mixed with the iron during emplacement, or they can be added to the iron as amendments prior to emplacement. Both scenarios provide greater confidence that contaminant reactions will be complete before the reactants exit the barrier and may allow the engineering of thinner barriers in situations constrained by cost or the presence of physical structures.

Introduction

When iron metal, Fe^0, is oxidized by corrosion processes to Fe^{2+} or Fe^{3+}, two or three electrons, respectively, are given up by the Fe. In aerobic environments oxygen is the primary acceptor of these electrons, hence the term "oxidation" of the iron. Other substances can also accept these electrons, and these substances become increasingly important as the oxygen in a system is depleted by ongoing corrosion reactions and is not rapidly replenished.

Recently it has been realized that such reactions can be used for contaminant remediation when reduction of the contaminant results in a more environmentally benign material. For example, the reduction of the mobile and toxic Cr(VI) to the much less toxic and immobilized Cr(III) precipitates (*1*–*3*) and the reductive dechlorination of highly chlorinated hydrocarbons to ethenes and ethanes have both been demonstrated to occur in aqueous systems containing iron metal (*4*, *5*). Therefore, a great deal of interest has been generated by the idea of incorporating scrap iron metal into permeable reactive subsurface walls that transect the flow paths of contaminant plumes. As the contaminated water enters the wall, reactions occur that would either transform the contaminant into an innocuous substance or immobilize the contaminant permanently in the wall. Water exiting the downgradient side of the wall would be free of the initial contaminant. Several of these walls have now been installed (*6*) and are assumed to be functioning, although there remains a scarcity of monitoring data.

In the design of a reactive barrier, many factors must be considered. These include the reaction rate for a given contaminant concentration per iron mass or surface area, the system geochemistry, and the hydrogeologic setting. These factors affect the residence time of the contaminated water in the wall necessary to achieve contaminant concentration goals. The ability to manipulate certain of these factors in an essentially passive manner would maintain cost-effectiveness while providing greater flexibility in design and greater confidence in achieving the remedial goals.

Simple batch and column experiments, consisting of water, iron, and contaminant, have shown that the reaction rates depend on the type of iron present and are linearly related to the available surface area for a given type of iron (*7*–*9*). Similar experiments, but containing actual aquifer mineral phases with simulated aquifer water, have shown that the geochemistry of some aquifer materials influences the reaction rates (*3*, *10*, *11*). An aquifer material from the U.S. Coast Guard Air Support Center near Elizabeth City, NC, was found to significantly enhance the reduction of chromate by a reactive type of Fe^0, referred to as Ada Iron and Metal (AI&M) iron. For these experiments a multiple regression model was needed to give the best fit of actual versus predicted chromate half-lives ($t_{1/2}$) for these systems (*11*). In addition to the mass of iron (mass ∝ surface area), this model incorporated the solid/solution ratio of the Elizabeth City aquifer material. Aquifer material from Cape Cod, Massachusetts, had a smaller effect on the reaction rates and a commercial silica sand even less. Studies have shown that these differences are not due to adsorption onto the aquifer materials (*12*).

Sieve, X-ray diffraction, and chemical analyses of these aquifer materials indicated that the primary difference between the Cape Cod and the Elizabeth City materials was a greater concentration of the aluminosilicate clay-sized minerals kaolinite, albite, and microcline in the Elizabeth City material (*12*, *13*). The silica sand was completely free of such components. It was hypothesized that the dissolution of one or more of these aluminosilicates resulted in the generation of solution protons. This would lower the pH to values more favorable for corrosion. The protons could also serve as electron acceptors at the iron surface, allowing the corrosion reactions to proceed more rapidly. A cyclic, multiple reaction electrochemical corrosion mechanism was proposed to explain the enhancement by aluminosilicate

* Author to whom correspondence should be addressed [telephone (702) 260-9434; fax (702) 260-9435; e-mail powell.associates@mci2000.com].
† Powell & Associates Science Services.
‡ U.S. Environmental Protection Agency.

S0013-936X(96)00734-1 CCC: $14.00 © 1997 American Chemical Society

TABLE 1. Aluminosilicate Minerals Used in the Experiments

mineral name or location	mineral type	surface area, m^2/g: determined, BET	surface area, m^2/g: standard value
KGa-2	kaolinite	20	23.5
SYN-1	synthetic micamontmorillonite	136	134
Branchville, CT	microcline feldspar (potassium aluminum silicate)	0.681	NA[a]
50 mi SE of Virginia City, MT	microcline feldspar (potassium aluminum silicate)	0.657	NA
Silas Moorefield Mine, Amelia Courthouse, VA	microcline feldspar, amazonite variety (potassium aluminum silicate)	0.812	NA
Bob Ingersoll Mine, Keystone SD	albite feldspar, cleavelandite variety, (sodium aluminum silicate)	ND[b]	NA
Portland, Middlesex Co., CT	albite feldspar, cymatolite variety (sodium aluminum silicate)—with muscovite mixture (mica)	0.864	NA

[a] NA, not available. [b] ND, not determined.

minerals (*11*). The proton generation occurring within this cycle was attributed to the following reactions:

$$\underset{\text{kaolinite}}{Al_2Si_2O_5(OH)_4(s)} + 5H_2O \rightarrow \underset{\text{silicic acid}}{2H_4SiO_4} + \underset{\text{gibbsite}}{Al_2O_3{\cdot}3H_2O(s)} \quad (1)$$

$$\underset{\text{gibbsite}}{Al_2O_3{\cdot}3H_2O(s)} + 2H_2O \rightarrow 2Al(OH)_4^- + \underset{\text{protons}}{2H^+} \quad (2)$$

$$\underset{\text{Fe surface}}{\equiv FeOH} + H_4SiO_4 \leftrightarrow \equiv FeOSi(OH)_3 + H_2O \quad (3)$$

$$\equiv FeOSi(OH)_3 \leftrightarrow \equiv FeOSiO(OH)_2^- + \underset{\text{proton}}{H^+} \quad (4)$$

These processes have important implications for designing in situ reactive wall treatment systems. If the contaminant transformation rates can be substantially increased, the residence time required in the wall will decrease, allowing more flexibility in the engineering design and confidence in the remedial action. In addition, if protons can be generated at the Fe^0 surfaces by such processes, dehalogenation reactions might be enhanced. Some researchers have shown much slower reduction of chlorinated ethenes at pH >8 (*14*). Rates of pentachlorophenol degradation by Fe^0 have also been found to decrease with increasing pH (*15*) and were faster using HCl-treated Fe^0 at pH 5. There have been numerous reports that the dechlorination of polychlorinated ethenes such as TCE slows with the formation of DCE isomers. Mass balance data are scarce, however, possibly due to adsorption of intermediates on the iron (*9*). Schreier and Reinhard (*16*) found that the transformations of both DCE and PCE ceased after 28–42 days in unbuffered systems and suggested a "threshold pH above which PCE transformation does not occur". The DCE results are probably attributable in part to the lower reduction potentials of the less chlorinated compounds (*9*), but typically these experiments have also shown pH values approaching or exceeding 9. Matheson and Tratnyek (*8*) found that the rate of carbon tetrachloride reduction slows with each dehalogenation step and seems to cease when methylene chloride is formed. They also showed a direct correlation between higher pH and reduced dechlorination rates in pH-buffered systems.

Corrosion processes have long been known to diminish in the pH range 9.5–12.5 (*17*). Additionally, the replacement moiety for the halogen atoms in these reductions is the hydrogen atom. It is possible that the dechlorination reactions slow at such high pH partly due to the paucity of hydrogen ions (ultimately resulting in scarce hydrogen atoms). Lending credence to these arguments, column tests with TCE have shown that the half-life of TCE (and daughter products) is significantly decreased in columns containing 52% Elizabeth City aquifer material and 48% iron relative to columns containing 100% iron (*18*).

TABLE 2. First-Order Chromate Half-Lives in Shaken Batch Bottle Experiments with Differing Aquifer Materials

aquifer material	chromate $t_{1/2}$, h
Elizabeth City + Fe	12
Cape Cod + Fe	26
silica sand + Fe	119
Fe with no aquifer material	>1000

[a] Each bottle contained 0.25 g of AI&M Fe, 26 mL of simulated aquifer water (pH 6.5, 0.86 mM $CaSO_4$, 7 mM NaCl), and, when present, 9 g of the aquifer material.

The primary objective of the current research was to test the hypothesis that aluminosilicate minerals were responsible for the increase in the reactivity of zero-valent iron. A further objective was to determine whether evidence for aluminosilicate dissolution could be obtained. Additional goals were to determine whether there were minimum and/or maximum aluminosilicate concentrations that affected the reaction rates and whether there were differences in the reactivities of differing aluminosilicate minerals.

Materials and Methods

The aluminosilicates chosen for study included kaolinite, montmorillonite, and a variety of feldspars. Table 1 identifies these materials. KGA-2 and SYN-1 were obtained from the Source Clay Minerals Repository, University of Missouri, Columbia, MO, whereas the five feldspars were purchased from Minerals Unlimited, Ridgecrest, CA. KGa-2 and SYN-1 were used as received. The feldspar minerals were received as individual rocks, which were pulverized to approximately −60 mesh using a Braun pulverizer. BET surface areas were determined by N_2 adsorption for the aluminosilicate materials.

Experiments to determine the effects of aluminosilicate materials on chromate reduction rates by Fe^0 were carried out using shaken batch bottle (SBB) techniques in a nitrogen-filled and oxygen-free glovebox. The basic setup of these SBB experiments has been described elsewhere (*11*). Varying masses of the aluminosilicates, from 0 to 0.5 g/26.3 mL of aqueous volume, were added to the SBBs to determine whether a relationship existed between the mineral mass and the rate of chromate reduction. Nine grams of relatively inert 10–20 mesh CSSI silica sand was used as an aquifer material in most of the experiments except for certain blanks. All samples contained 0.25 g of water-washed iron filings obtained from AI&M. Samples were prepared in duplicate.

A chromate reduction experiment using a "field mix" was carried out using the SBB protocol (*11*). The field mix is a mixture that was used in a "fence" of reactive boreholes at the U.S. Coast Guard Air Support Center, Elizabeth City, NC, as a pilot-scale test that intercepted a mixed chromate–TCE plume (*19*). The mix consisted of 25% by volume each of AI&M iron, Master Builder's Supply iron, Elizabeth City aquifer

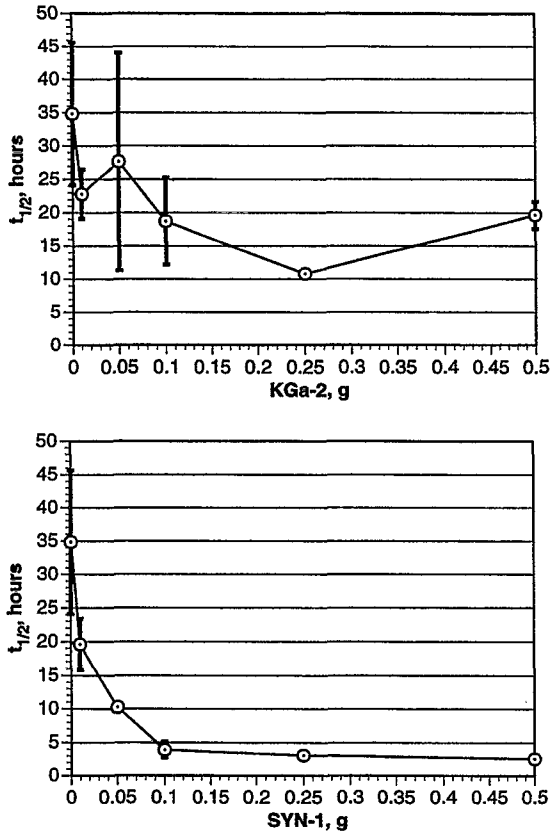

FIGURE 1. Effects of varying masses of aluminosilicate clays KGa-2 kaolinite (a, top) and SYN-1 montmorillonite (b, bottom) on the solution $t_{1/2}$ (⊙, first-order average) of chromate in hours at a constant 0.25 g of Fe^0 mass. The circles are $t_{1/2}$ means of duplicates; the line endpoints represent the $t_{1/2}$ for each of the duplicates.

material, and pea gravel. This batch experiment was similar to the others except that the mixture was added from 0 to 2.0 g. No additional aquifer materials or minerals were added, with the exception of one set of additional samples that contained 1.0 g of field mix and 0.1 g of SYN-1 montmorillonite.

SBB experiments were also used to evaluate the dissolution of the aluminosilicates over a pH range representative of those previously observed in experiments on chromate reduction by iron corrosion. Batch experiments were begun in Oak Ridge polyallomer centrifuge tubes using 38 mL of simulated Elizabeth City aquifer water (7 mM NaCl, 0.86 mM $CaSO_4$) that had been preadjusted to pH values of 6.5, 7.5, 8.3, and 9.2. No Fe^0 was present in these pH-adjusted samples. Adjustments to pH were made using 0.1 M NaOH and 0.1 M $HClO_4$ solutions. Upon addition of 0.42–0.44 g of aluminosilicate materials (duplicate samples) to the tubes, the tubes were vigorously shaken and allowed to set for 15 min, at which time pH was checked. The pH was then adjusted with the appropriate acid or base solution, the shaking was repeated, and the tubes were again allowed to set for 15 min. This process was repeated initially and at each sampling interval until the pH was stable within 0.1 pH unit for two consecutive 15 min periods. This resulted in a relatively consistent and narrow range of pH variation over the course of the experiments.

Tubes were also prepared for the dissolution experiments that contained the solution, aluminosilicates, and 1.0 g of AI&M Fe^0 or 1.0 g of AI&M Fe^0 plus chromate. These were not pH adjusted but allowed to attain their natural reaction pH. All tubes were then placed on a rotating shaker at approximately 300 rpm. Sampling intervals were at 24, 48, 96, and 192 h from the solid phase addition. At the end of

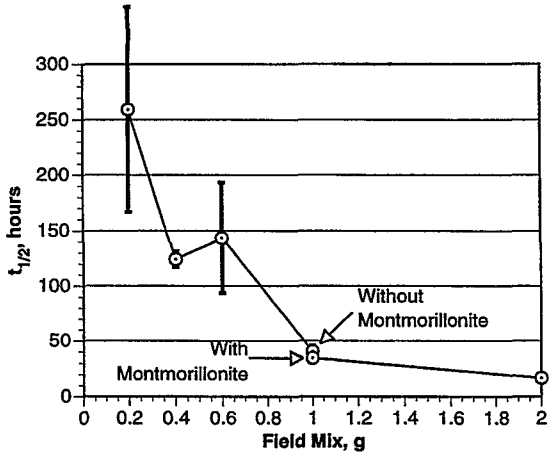

FIGURE 2. Solution chromate $t_{1/2}$ (⊙, first-order average) at various masses of Elizabeth City field mix and the effect of adding 0.1 g of SYN-1 montmorillonite at the 1 g field mix mass. The circles are $t_{1/2}$ means of duplicates; the line endpoints represent the $t_{1/2}$ for each of the duplicates.

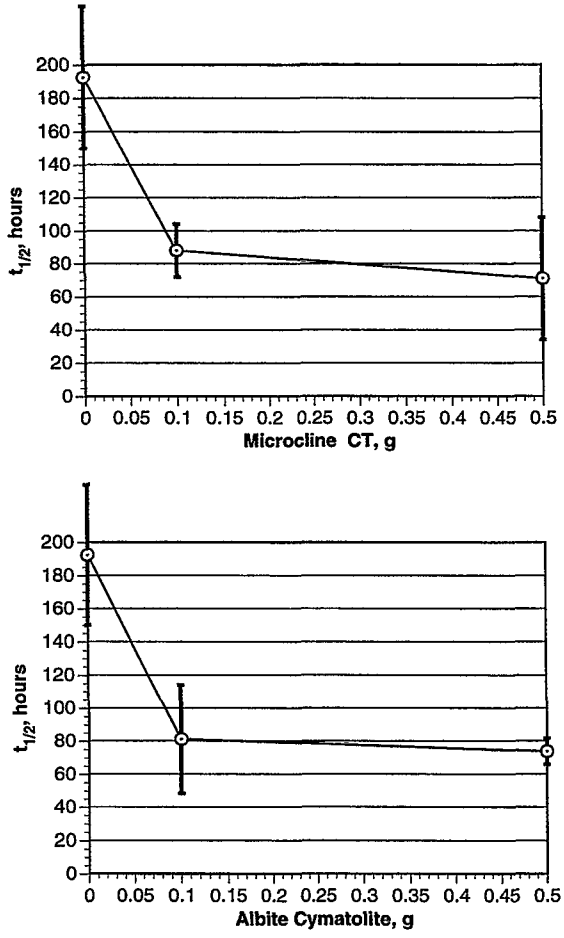

FIGURE 3. Effects of varying masses of aluminosilicate feldspars microcline CT (a, top) and albite cymatolite (b, bottom) on the solution $t_{1/2}$ (⊙, first-order average) of chromate in hours at a constant 0.25 g of Fe^0 mass. The circles are $t_{1/2}$ means of duplicates; the line endpoints represent the $t_{1/2}$ for each of the duplicates.

each sampling interval the tubes were removed from the glovebox and centrifuged at 10 000 rpm for 60 min. Eight milliliter sample aliquots were removed without disturbing the sediment and filtered through 0.05 μm pore diameter Nuclepore membrane filters to remove any suspended colloidal phases. The filtrate was submitted for Si and metals

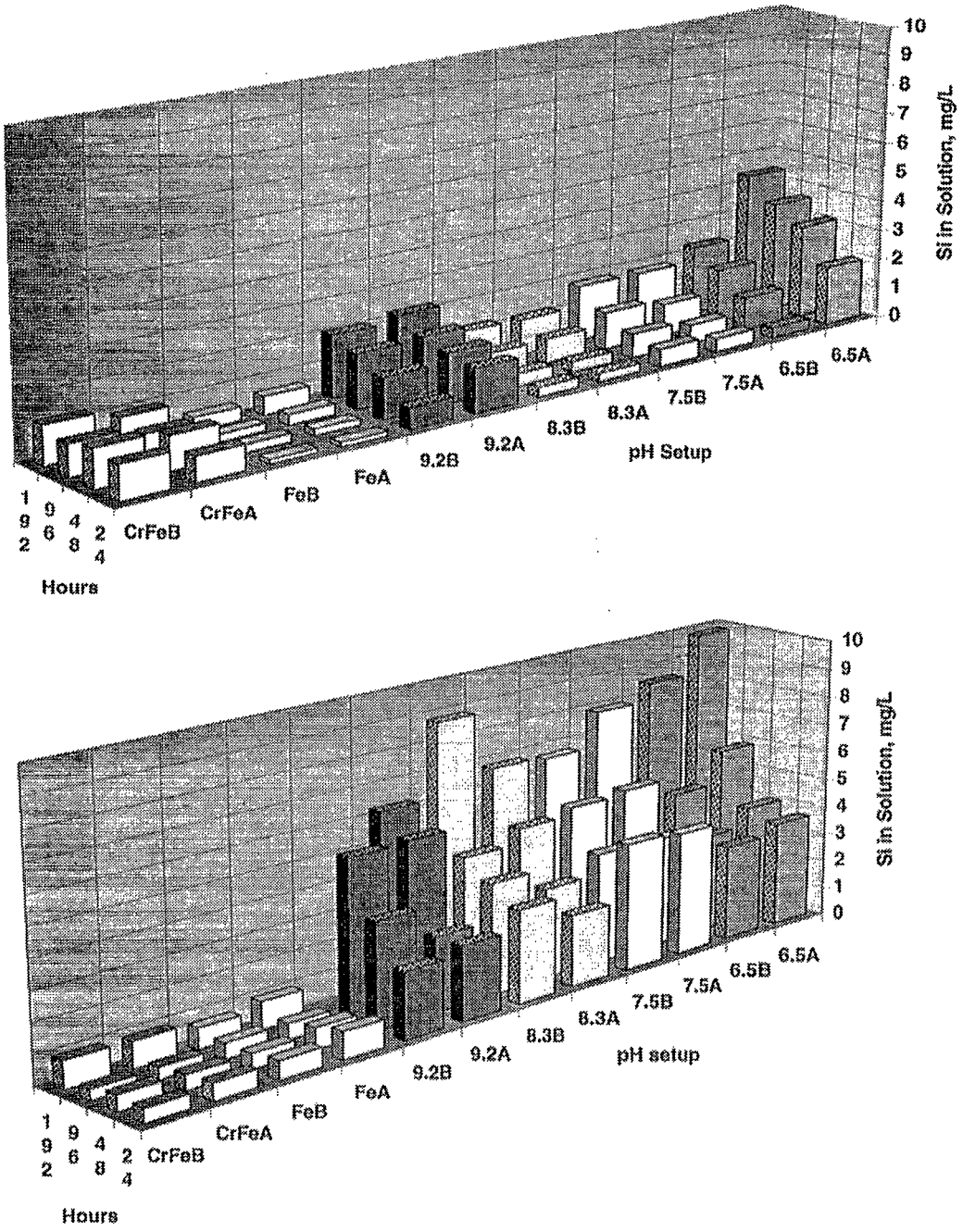

FIGURE 4. Si in solution dissolved from KGA-2 kaolinite (a, top) and SYN-1 montmorillonite (b, bottom) over a range of constant pH values and in the presence of iron (Fe samples) and chromate plus iron (CrFe samples) at four time intervals .

analysis by ICP-AES. The sediments were then resuspended and returned to the glovebox; the pH was checked and adjusted as given above, and the sediments were returned to the shaker.

Results and Discussion

Aluminosilicate Effects on Chromate Reduction. Chromate half-life data from prior batch experiments are shown in Table 2 (*12*). The only difference among these was the source of the aquifer material. These and other results, combined with mineralogic differences among the aquifer materials, led to the hypothesis that aluminosilicate minerals enhanced chromate reduction. Experiments with specific aluminosilicate minerals (Table 1) tested this hypothesis.

Parts a and b of Figure 1show the effects of varying masses of KGa-2 kaolinite and SYN-1 mica montmorillonite, respectively, on the solution chromate $t_{1/2}$ in hours in these systems based on pseudo-first-order kinetics. The zero value on the abscissa indicates that no aluminosilicate clay was added and provides the $t_{1/2}$ due only to the presence of the Fe^0 in the system. For these plots, the circles indicate the $t_{1/2}$ mean of the duplicate samples, whereas the endpoints of the bars represent the $t_{1/2}$ of each duplicate, not 95% confidence intervals. Sorption studies (not depicted) were carried out using 0.1 and 0.5 g masses of both kaolinite and montmorillonite. In the absence of Fe^0 no significant loss of chromate from solution due to sorptive processes was detected.

The kaolinite duplication (Figure 1a) is poor at masses of kaolinite <0.1 g. This is probably because heterogeneities in the reactivities of the small (0.25 g) iron masses overwhelmed the effects of the very small kaolinite additions. At kaolinite

masses of 0.1–0.5 g it appears that some positive effect on the chromate reduction rate has occurred, reducing the $t_{1/2}$ from a mean of 35 h to between 10 and 20 h.

The heterogeneity of the iron had less effect on the reduction enhancement by montmorillonite (Figure 1b). Even at very low concentrations of SYN-1 (0.01 g/26 mL) a reduction in mean $t_{1/2}$ from 35 h to <20 h was observed. At 0.10 g of SYN-1 the $t_{1/2}$ has decreased to approximately 4 h, with only minor additional decreases at 0.25 and 0.50 g. This asymptotic relationship of montmorillonite mass versus $t_{1/2}$ seems to indicate a maximum effective enhancement concentration for addition of the aluminosilicate. This diminishing return is probably related to the available iron surface and the maximum rate at which it can undergo corrosive dissolution due to other limiting factors, such as mass transport and diffusion. That is, if previous hypotheses about contribution of protons via aluminosilicate dissolution processes are correct, the availability of the proton as an electron acceptor no longer seems to be reaction-limiting when montmorillonite is available at levels of ≥0.1 g in these systems.

This diminishing enhancement of chromate reduction beyond some maximum effective concentration of aluminosilicate is supported by Figure 2, which implies that the Elizabeth City aquifer material minerals were intrinsically capable of reaching this maximum rate of chromate reduction without augmenting the aluminosilicate mineral concentration. This plot depicts the chromate reduction $t_{1/2}$ versus the mass of field mix. The $t_{1/2}$ decreased with increasing mass of field mix (which also added more iron with each mass increase). However, at the level of 1 g of field mix/26.3 mL of solution, adding 0.1 g of SYN-1 montmorillonite was ineffective for increasing the chromate reduction rate beyond that already present in the mix from the naturally occurring aluminosilicates.

Preliminary experiments were performed on all five feldspars listed in Table 1 to determine their effects on chromate reduction by Fe^0. Although differences in enhancement among the five were not large, the microcline feldspar from Branchville, CT and the albite, cymatolite variety, also from Connecticut, seemed to be the best enhancers. These were chosen for further experimentation. Figure 3 shows that solution chromate $t_{1/2}$ was reduced by the presence of the feldspars in these experiments, from a mean of about 192 h to means of 71 and 74 h at the 0.5 g of feldspar level. Again, not much enhancement in the reactions was seen above 0.1 g of aluminosilicate addition, and sorption experiments showed no sorption of chromate by the aluminosilicate.

In summary, every tested aluminosilicate mineral enhanced the rate of chromate reduction in systems of zero-valent iron, with no evidence whatever of simple adsorption of the chromate from solution.

Aluminosilicate Dissolution in Nonequilibrium Systems. Since data indicated that a broad variety of aluminosilicate minerals was capable of enhancing chromate reduction by Fe^0, it was necessary to determine whether evidence of aluminosilicate dissolution could be found in these systems. Such evidence would support the dissolution processes given in eqs 1 and 2.

Aluminosilicate dissolution tests were carried out at maintained pH values of 6.5, 7.5, 8.3, and 9.2 with no Fe^0 present and in pH-unadjusted samples containing Fe^0 and Fe^0 plus chromate. Parts a and b of Figure 4depict the Si in solution results versus pH at times (as axis categories) of 24, 48, 96, and 192 h for KGa-2 kaolinite and SYN-1 montmorillonite, respectively. The feldspar data are not shown, but solution Si concentration results were midway between the kaolinite and montmorillonite data. It is apparent that mineral dissolution has occurred in these systems since the concentration of Si in solution increases at every time interval at every pH. The Si values for the SYN-1 montmorillonite

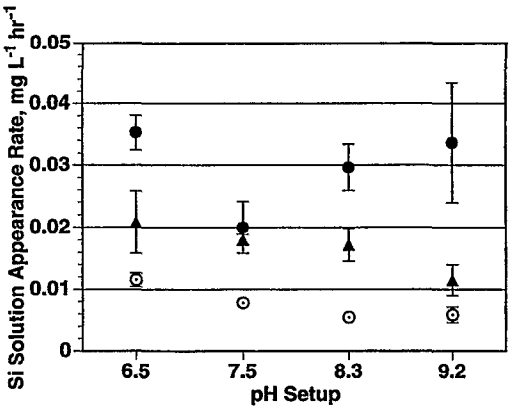

FIGURE 5. Zero-order rate of Si appearance in solution at each constant pH for each type of mineral: (●) SYN-1; (⊙) KGa-2; (▲) microcline CT.

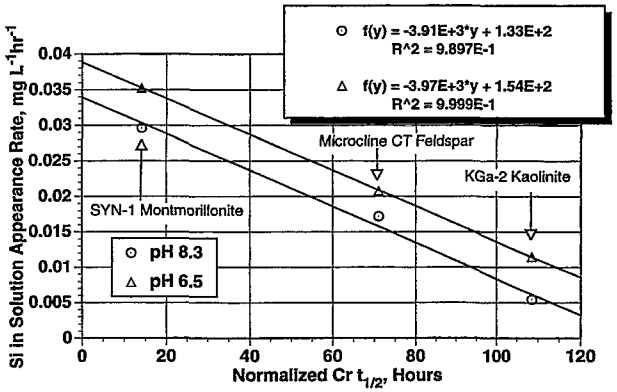

FIGURE 6. Zero-order rate of Si appearance in solution at pH 6.5 and 8.3 for each mineral versus the normalized $t_{1/2}$ for chromate removal from solution by Fe^0 in the presence of the mineral.

(Figure 4b) are significantly higher than those for the KGa-2 kaolinite (Figure 4a), indicating greater dissolution for this mineral. Such an increase could be anticipated for the montmorillonite since smectite clays are known to expand their interlayer spacing (swell) when wet. This expansion would increase the water-exposed surface area of the clay far beyond that determined on the dry material (Table 1), increasing the potential dissolution rate. Kaolinitic clays do not expand significantly when wet; hence, this material released much less Si to the solution per the same mass of clay. This difference in dissolution rate could also account for the much greater enhancement in CrO_4^{2-} reduction when montmorillonite is present rather than kaolinite.

Interestingly, the Fe^0-containing, non-pH-adjusted samples FeA, FeB, CrFeA, and CrFeB show less free Si in the solution for the KGa-2 system and much less free Si for the SYN-1 system (Figure 4). These data appear to be anomalous, but eq 3 predicts this result. Coordination of the free silicic acid to the iron oxyhydroxide rusts formed from the corrosion process would lower the Si solution concentration. Since there is no Fe in the pH-maintained samples, this removal does not occur.

The appearance of Si in solution is best fit, at all four pH-maintained values, by zero-order kinetics with respect to the Si. Figure 5 plots the reaction rates of Si appearance in milligrams per liter per hour for each pair of duplicates and their means for each aluminosilicate mineral at each tested pH. This plot depicts the intermediate position of the feldspar microcline CT with respect to dissolution for the same mineral mass. This feldspar had nearly 30 times less surface area per gram than the kaolinite (Table 1), showing that dry surface area alone is not a reliable indicator of this reactivity.

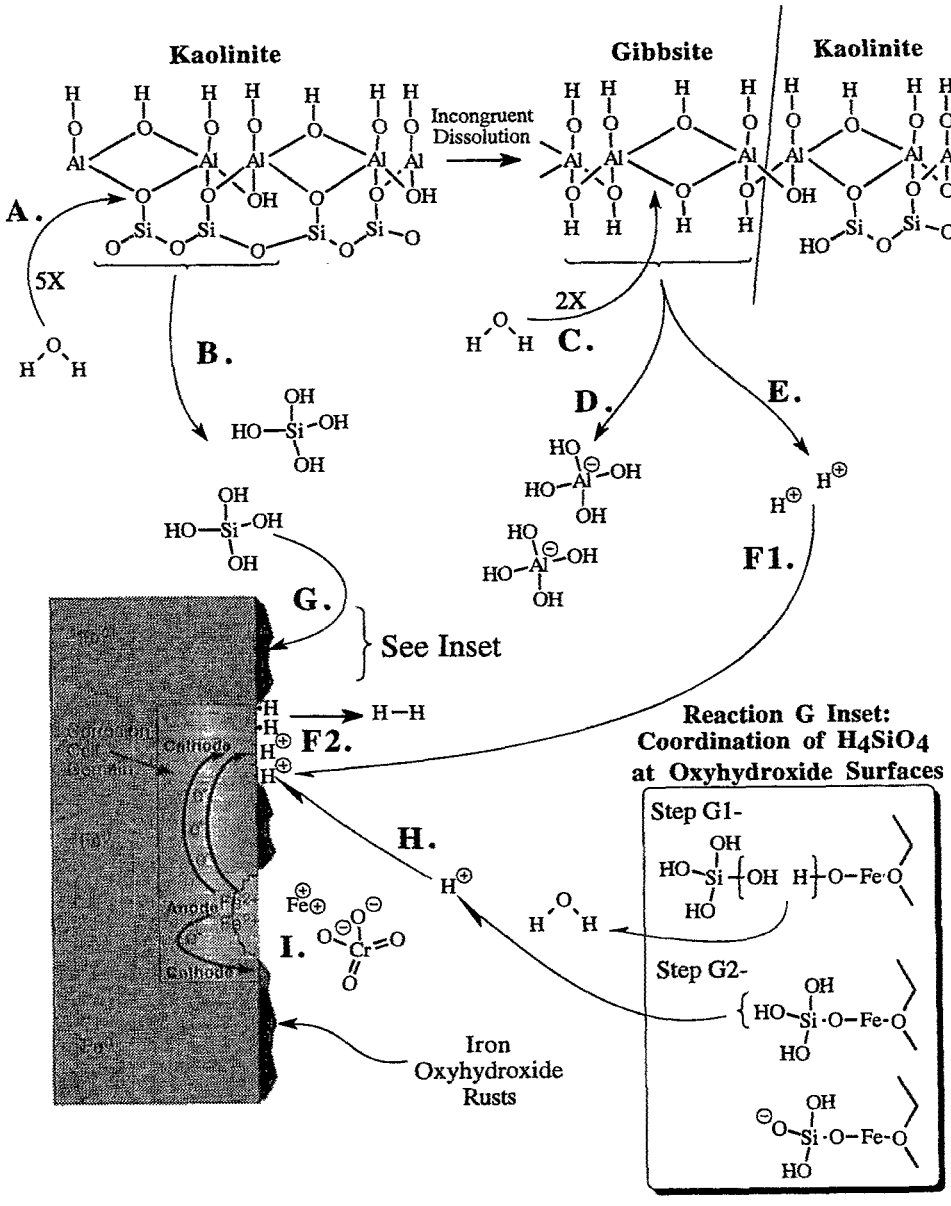

FIGURE 7. Schematic diagram of the main features of the proposed cyclic aluminosilicate dissolution/proton generation reactions for contaminant remediation using Fe^0.

In fact, when surface area is considered, it becomes apparent that the feldspar was the most reactive of the minerals with respect to mineral dissolution. The SYN-1 montmorillonite had nearly 200 times the dry surface area of the feldspar but showed only about twice the rate of solution Si appearance at pH values from 6.5 to 9.2. This observation becomes even more pronounced when the swelling of the montmorillonite under fully saturated conditions is considered. If the fully expanded montmorillonite surface area is up to 800 m^2/g (*20*), then up to 1100–1200 times the feldspar surface area was exposed to aqueous dissolution. Therefore, the feldspar surfaces are more reactive for an equivalent amount of surface area. This is because the feldspars are relatively unweathered primary minerals, whereas montmorillonite and kaolinite are secondary minerals derived from the weathering of the primary minerals. The solubility sequence for these minerals under most conditions appears to be microcline > montmorillonite > kaolinite (*21*), which is also, in general, the weathering sequence found in soil development (*20*).

Coordination of Chromate Reduction and Aluminosilicate Dissolution Processes. The mean zero-order Si dissolution reaction rate for each aluminosilicate at pH values of 6.5 and 8.3 was plotted versus the normalized chromium reduction mean $t_{1/2}$ value determined for the 0.42–0.44 g aluminosilicate samples from the aluminosilicate effects experiments (Figure 6). These two pH values were chosen to bracket a typical range for corrosion systems of Fe^0 and Elizabeth City aquifer material or added aluminosilicates (typically pH from 7.2 to 7.8). The 0.42–0.44 g of aluminosilicate $t_{1/2}$ values were chosen to correspond most closely with the mass of mineral used in the dissolution experiments. It was necessary to normalize the SYN-1 and KGa-2 values for Cr $t_{1/2}$ to the microcline CT $t_{1/2}$ values before plotting. This was because the initial AI&M iron had been used up. A different batch of AI&M iron that yielded much lower reactivity was used for the microcline experiments. The $t_{1/2}$ of the second batch of iron when no aluminosilicate was present (Figure 3, 192.5 h) was divided by the $t_{1/2}$ of the original batch of iron when no aluminosilicate was present (Figure 1, 34.8 h). The large difference in these $t_{1/2}$ values re-emphasizes the large influence of iron type in these systems. The calculated factor was then used to correct the KGa-2 and SYN-1 $t_{1/2}$ to higher values, as though they had been run with

the same AI&M Fe as the feldspar. Figure 6 shows a linear relationship between the chromate reduction rate and the mineral dissolution rate at each pH value. This is evidence that the aluminosilicate dissolution has a direct impact on chromate reduction rates: the more rapidly Si appears in solution, the faster the CrO_4^{2-} is reduced.

Figure 7 depicts the essential components of a proposed cyclic reaction framework containing eqs 1–4, using the relatively simple structure of kaolinite to represent an aluminosilicate mineral phase. Although the figure is drawn in an open fashion, in fact, all of the aspects of this diagram would be in intimate juxtaposition and contact. Reaction A shows the cleaving of the tetrahedral kaolinite layer of the mineral by five water molecules. This results in the dissolution of two molecules of H_4SiO_4 (silicic acid, eq 1, reaction B). Further attack by two water molecules on the resultant octahedral gibbsite layer (eq 2, reaction C) yields two molecules of $Al(OH)_4$ (reaction D) and two protons (reaction E). These protons are then capable of lowering the pH (reaction F1), as well as coordinating with the cathodic regions of corrosion cell domains on the Fe^0 surface and accepting electrons, thereby forming monoatomic hydrogen and the diatomic gas, H_2 (reaction F2). The silicic acid from reaction B can coordinate with the iron oxyhydroxide rusts on the surface of the Fe^0 (reaction G). This involves a series of reactions that are illustrated in the figure inset. In step G1 (eq 3) a dehydration occurs, coordinating the Si atom with O on the iron oxyhydroxide surface. Step G2 is a deprotonation (eq 4), resulting in a negatively charged silicate surface structure on the oxyhydroxide and releasing a proton to the solution. This proton is then free to lower pH and react, potentially by accepting an electron at the cathodic surface of the Fe^0 (reaction H).

Thus, for every two silicon tetrahedra removed from the kaolinite surface, four protons can be generated. This proton-generating mechanism is cyclic due to the coordination of the silicic acid with the oxyhydroxide surfaces. As the solution H_4SiO_4 becomes depleted, solution disequilibrium should continue since the silicic acid concentration remains low, resulting in ongoing mineral dissolution. Although it has not been studied in the laboratory, it is possible that this cycle of proton generation could continue until the initial aluminosilicate mineral phase is depleted.

The availability of the protons as electron acceptors results in increased electron transfer within the metal. This causes an increase in the corrosion rate, freeing Fe^{2+} in the anodic regions of the corrosion cell domain and enhancing the reduction of chromate (Figure 7, Reaction I) when it is present. As these reactions occur, monoatomic hydrogen could become increasingly available at the iron surface for reductive dechlorination reactions. Figure 8 illustrates the potential benefit for the dechlorination of TCE at the Fe surface, showing electron transfers to both TCE and a proton followed by reaction of the resultant monoatomic hydrogen and the organic radical to yield *cis*-1,2-DCE and a chloride ion. Irrespective of whether the reductive dechlorination consists of two electron transfers (as depicted) or the simultaneous transfer of two electrons preferred by Roberts et al. (*22*), increasing the corrosion rates should increase the contaminant transformation rate. It seems reasonable to conjecture that if the protons are increasing the corrosion rate due to accepting electrons, the increased availability of monoatomic hydrogen on the cathodic surface should enhance organohalide transformations. Competition between the organohalides and the protons for these electrons is probably fairly unimportant since the concentrations of both will typically be very low relative to the Fe surface area. More research is needed to determine the exact mechanisms of these reactions.

The data show that proton generation by aluminosilicate mineral dissolution increases the rate of contaminant transformations by zero-valent Fe corrosion reactions. These

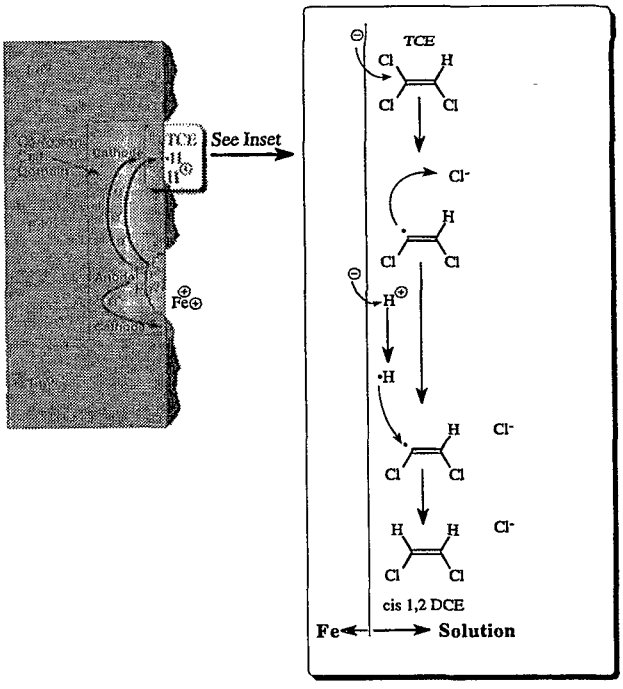

FIGURE 8. Schematic diagram of a potential enhancement to reductive dechlorination of TCE at the Fe cathodic surface due to reduction of protons in proximity to the TCE. Inset: Reductive dechlorination of TCE at the cathodic surface of the corroding Fe.

minerals may be naturally occurring within the geochemical milieu of a site, allowing them to be readily mixed with the iron as the reactive barrier is installed. Alternatively, if no native aluminosilicate minerals are present, they could be added as amendments to the iron prior to placing it in the ground. If amending, the choice of mineral has a large impact on the enhancement. For chromate remediation, the effects were in the order montmorillonite > feldspar > kaolinite for equivalent masses. All three minerals approached their maximum enhancement level in the experiments at 0.1 g of aluminosilicate addition to 0.25 g of Fe^0 per 26 mL. Increasing the aluminosilicate beyond this proportion did not gain much in reactivity and might contribute to premature blockage of the pore space within a reactive barrier due to increasing the barrier's particle size heterogeneity. Such blockage could eventually reduce water flow through the wall. This is already considered to be a potential problem, even for unamended systems, due to the formation of corrosion precipitates. Because of this concern, montmorillonite will not be the best amendment choice since it is a highly swelling clay that could readily plug the pore spaces. Feldspar minerals do not have the undesirable swelling property and should be the best choice from among the tested minerals.

It is apparent that site-specific geochemistry, in addition to the type of iron used, the contaminant species, and their concentrations can have a large impact on in situ remediation processes using zero-valent iron. Information about such impacts and their mechanisms of influence can be used to design better treatment walls and increase confidence in their effectiveness.

Acknowledgments

Although the research described in this paper was funded by the U.S. Environmental Protection Agency under Contract 68-C3-0322 to ManTech Environmental Research Services Corp., Ada, OK, and under in-house research programs, it has not been subjected to Agency review and therefore does not necessarily reflect the views of the Agency, and no official endorsement should be inferred. We thank Mr. Steve Weber

of the Oklahoma Geological Survey (OGS) for his assistance and the use of OGS equipment in the preparation of the feldspar minerals. We also thank Sharon Hightower, Jeri Lynn Anderson, and Nohora Vela of ManTech Environmental Research Services Corp. and Don Clark (now retired) of the U.S. Environmental Protection Agency for the experiments they carried out and the analyses they performed in support of this research.

Literature Cited

(1) Gould, J. P. *Water Res.* **1982**, *16*, 871–877.
(2) Blowes, D. W.; Ptacek, C. J. In *Proceedings of the Subsurface Restoration Conference, Third International Conference on Ground Water Quality Research*; National Center for Ground Water Research: Dallas, TX, 1992; pp 214–216.
(3) Powell, R. M.; Puls, R. W. Metal Speciation and Contamination of Aquatic Sediments Workshop, Jekyll Island, GA, 1993.
(4) Gillham, R. W.; O'Hannesin, S. F. *Ground Water* **1991**, *29*, 752.
(5) Gillham, R. W.; Burris, D. R. In *Proceedings from the Subsurface Restoration Conference*; Rice University, Department of Environmental Science and Engineering, Houston, Texas: Dallas, TX, June 21–24, 1992; pp 66–68.
(6) Yamane, C. L.; Warner, S. D.; Gallinatti, J. D.; Szerdy, F. S.; Delfino, T. A.; Hankins, D. A.; Vogan, J. L. In *Abstracts, 209th National Meeting of the American Chemical Society*, April 2–7, Division of Environmental Chemistry: Anaheim, CA; American Chemical Society: Washington, DC, 1995; pp 792–795.
(7) Gillham, R. W.; O'Hannesin, S. F. *Ground Water* **1994**, *32*, 958–967.
(8) Matheson, L. J.; Tratnyek, P. G. *Environ. Sci. Technol.* **1994**, *28*, 2045–2053.
(9) Sivavec, T. M.; Horney, D. P. In *Abstracts, 209th National Meeting of the American Chemical Society*, April 2–7, Division of Environmental Chemistry; Anaheim, CA; American Chemical Society: Washington, DC, 1995; pp 695–698.
(10) Powell, R. M.; Puls, R. W.; Paul, C. J. In *Proceedings Water Environment Federation, Innovative Solutions for Contaminated Site Management*; Water Environment Federation: Miami, FL, March 6–9, 1994; pp 485–496.
(11) Powell, R. M.; Puls, R. W.; Hightower, S. K.; Sabatini, D. A. *Environ. Sci. Technol.* **1995**, *29*, 1913–1922.
(12) Powell, R. M. M.S., The University of Oklahoma, Norman, OK, 1994.
(13) Petrie, L.; Marozas, D.; Paulson, S.; Boucher, M. Report to EPA R. S. Kerr Environmental Research Laboratory on Characterization of Elizabeth City Site Samples; U.S. Department of the Interior, Bureau of Mines, 1993.
(14) Senzaki, T.; Kumagai, Y. *Kogyo Yosui* **1988**, *357*, 2–7.
(15) Ravary, C.; Lipczynska-Kochany, E. In *Abstracts, 209th National Meeting of the American Chemical Society*, April 2–7, Division of Environmental Chemistry, Anaheim, CA, American Chemical Society: Washington, DC, 1995; pp 738–740.
(16) Schreier, C. G.; Reinhard, M. *Chemosphere* **1994**, *29*, 1743–1753.
(17) Pourbaix, M. *Atlas of Electrochemical Equilibria in Aqueous Solutions*; Pergamon Press: Oxford, U.K., 1966.
(18) O'Hannesin, S. Internal Draft Report to U.S. EPA, Waterloo Center for Ground Water Research, University of Waterloo, Waterloo, ON, Aug 1995.
(19) Puls, R. W.; Paul, C. J.; Powell, R. M. In *The Fourth Great Lakes Geotechnical and Geoenvironmental Conference, In-Situ Remediation of Contaminated Sites*; Reddy, K. R., Ed.; University of Illinois at Chicago: Chicago, IL, 1996; pp 23–37.
(20) Bohn, H. L.; McNeal, B. L.; O'Connor, G. A. *Soil Chemistry*; Wiley: New York, 1979; p 329.
(21) Rai, D.; Kittrick, J. A. In *Minerals in Soil Environments*; Dixon, J. B., Weed, S. B., Eds.; Soil Science Society of America: Madison, WI, 1989; pp 161–198.
(22) Roberts, L. A.; Totten, L. A.; Arnold, W. A.; Burris, D. R.; Campbell, T. J. *Environ. Sci. Technol.* **1996**, *30*, 2654–2659.

Received for review August 27, 1996. Revised manuscript received April 16, 1997. Accepted April 23, 1997.[⊗]

ES9607345

[⊗] Abstract published in *Advance ACS Abstracts,* June 15, 1997.